Nido-cage···π Bond: A New Non-Covalent Interaction

Deshuang Tu,[a] Hong Yan,*[a] Jordi Poater,*[b,c] Miquel Solà*[d]

[a]State Key Laboratory of Coordination Chemistry, Nanjing University, Nanjing 210023, P. R. China

[b]Departament de Química Inorgànica i Orgànica & Institut de Química Teòrica i Computacional (IQTCUB), Universitat de Barcelona, Martí i Franquès 1-11, 08028 Barcelona, Catalonia, Spain

[c]ICREA, Pg. Lluís Companys 23, 08010 Barcelona, Spain

[d]Institut de Química Computacional i Catàlisi and Departament de Química, Universitat de Girona, C/ Maria Aurèlia Capmany, 69, 17003 Girona, Catalonia, Spain

KEYWORDS: Non-covalent interaction; carborane; multicenter multielectron bonding; *nido*-cage···π interaction; aggregation-induced emission; crystal engineering; density functional theory; energy decomposition analysis

ABSTRACT: Exploration and comprehension of new chemical bonding is one of the central tasks in chemistry. To date, non-covalent interactions based on σ- and π-bonding molecules such as hydrogen bonds and π···π interactions have been extensively investigated. However, the research on chemical bonding involving multicenter multielectron skeletons like boron clusters is much less reported. Here, a new type of non-covalent interaction, *nido*-cage···π bond, is discovered based on the boron cluster $C_2B_9H_{12}^-$ and an aromatic π system. The X-ray diffraction studies indicate that the *nido*-cage···π bonding presents the same parallel-displaced or T-shaped geometries as a π···π interaction does. The contacting distance between the cage and the π ring varies with the type and the substituent of the aromatic ring. The quantum chemical calculations reveal that this *nido*-cage···π non-covalent interaction shares a similar nature to the conventional anion···π or π···π bond found in classical aromatic ring systems. Besides, effective electronic communication between the boron cluster and the π unit is observed through the *nido*-cage···π interaction, which leads to unique photophysical properties such as both aggregation-induced emission in the amorphous state and aggregation-caused quenching in the crystalline state in one molecule. This demonstrates distinct emission behaviors from the conventional organic luminogens. The present work not only offers an overall understanding on this new non-covalent interaction, but also opens a door to investigate its properties and further applications.

Introduction

Exploration and discovery of new chemical bonding is of great importance for chemistry, materials, catalysis, and related fields.[1] Non-covalent interactions have played significant roles in many forefront areas of modern chemistry such as from materials design to molecular biology.[2] As such, the investigation on the physical origin and the scope of such interactions as hydrogen bonds, halogen bonds, and π···π interactions has been tremendously strengthened (Figure 1a).[3] However, non-covalent interactions involving multicenter multielectron skeletons such as three center-two electron (3c-2e) bonding clusters are much less documented[4] (Figure 1b).

Appealing in theory and experimentally proven to exist, non-covalent interactions involving π-bonding aromatic surfaces are easily formed in aggregation state and even in gas phase due to their conjugated electronic structures.[5] These classical intermolecular interactions are stabilized by significant binding energies. For example, the π···π interaction of benzene dimers shows two isoenergetic structures (T-shaped (edge-to-face) and parallel-displaced) with interaction energies of -2.4 and -2.8 kcal/mol.[6] The attractive π···π interactions not only influence the crystal packing structures of organic molecules, but also tune the three-dimensional structures of proteins and DNA.[5] As the analogues of aromatic rings, three-dimensional boron clusters such as carboranes have been investigated for over half century in materials, catalysis, energy, pharmaceutical, medicinal studies, etc.[7] Nonetheless, the non-covalent bonding research involving boron-cluster skeletons is scarcely reported[4] even though the boron clusters show similar features[8] such as chemical reactivity and aromaticity to the conventional aromatic rings. Up to now, it remains unexplored whether and/or how such a new type of non-covalent interaction, denoted as *nido*-cage···π bond between a boron cluster and a π ring as shown in Figure 1b, could be established with specific bonding strength and geometric preference. Herein, to address this goal, we started from a rational design of *nido*-carborane-based derivatives, which are shown in Figure 1b. As indicated by X-ray crystallography, the contacting distance from centroid to centroid of the *nido*-cage···π bond is in the range 4.422 – 5.904 Å, depending on the planar π systems and the substituents of the aromatic rings. The *nido*-cage···π bond drives to form either parallel-displaced or T-shaped geometries between the *nido*-carboranyl cage and an aromatic ring, having the same bonding modes as the conventional π···π

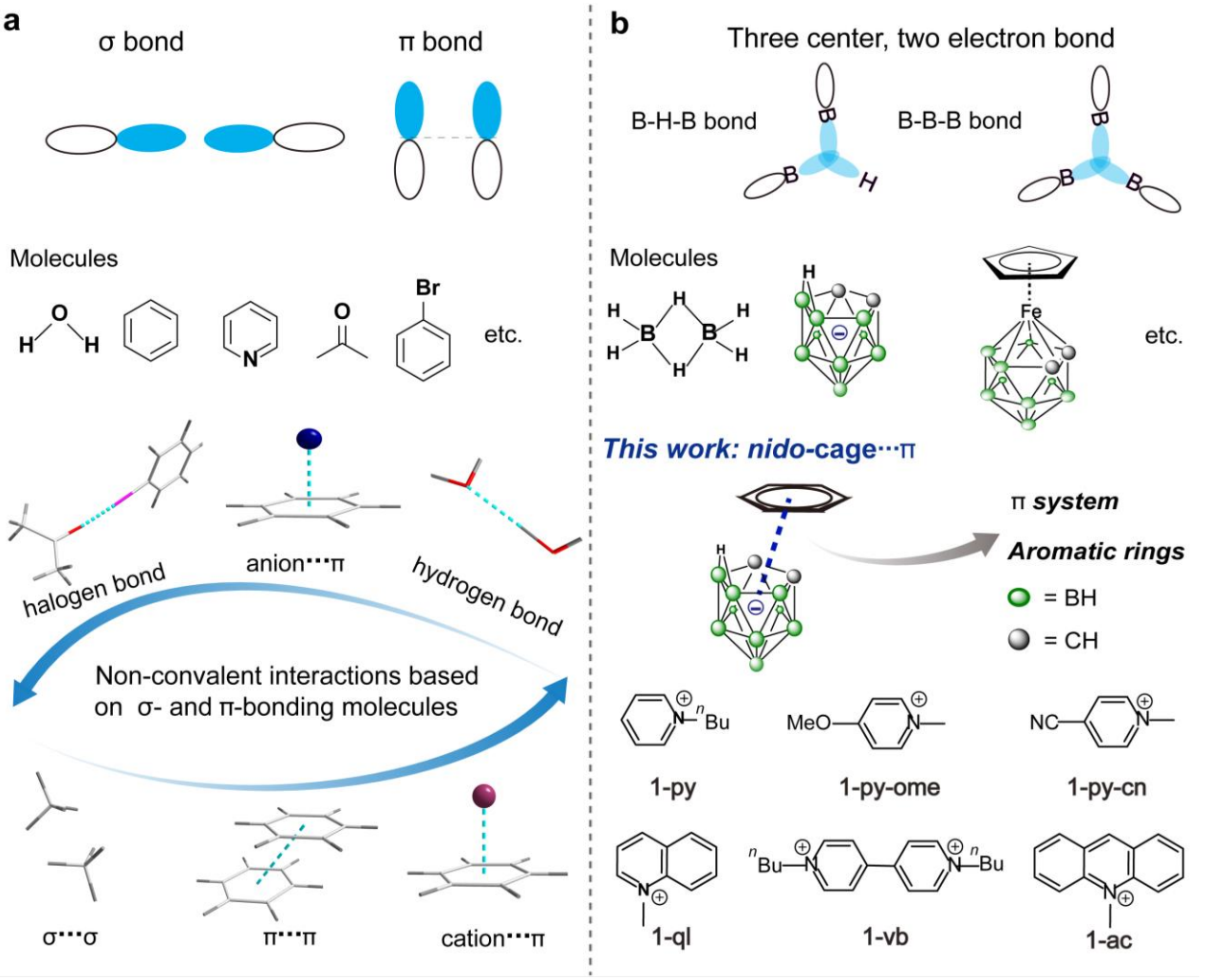

Figure 1. a) Non-covalent interactions based on σ- and π bonding molecules. b) Proposed *nido*-cage···π interaction between *nido*-carborane and aromatic rings.

interaction. Theoretical calculations prove that the boron cluster-based bond has a similar nature to that of anion···π and π···π bonds in aromatic systems. Moreover, the *nido*-cage···π interaction enables to induce variable photophysical properties such as aggregation-cause quenching (ACQ) and aggregation-induced emission (AIE) in one molecule. Therefore, the discovery of this *nido*-cage···π bond may open the door to a new research avenue for supramolecular chemistry, luminescent materials, and other potential applications.

Results and discussion

Synthesis and characterization of *nido*-cage…π interaction

As a proof of concept to validate the *nido*-cage···π interaction, various aromatic rings like pyridinium were chosen to make ionic pairs with *nido*-carborane ($C_2B_9H_{12}^-$) (Figure 1b). The target compounds can be synthesized through ion exchange in high yields (Schemes S1 and S2). The structures were carefully characterized by ^{1}H-, ^{13}C-, ^{11}B-NMR, mass spectrometry, and X-ray diffraction (Figure S2). All data indicate that *nido*-carborane can be incorporated to be part of certain ionic pairs. In solution, the chemical shifts of the *nido*-carboranyl moiety are not affected by the cations, as shown by both ^{11}B- and ^{1}H-NMR when compared to the control compound **1-et** (Figure S1). Obviously, the attractive interaction for the ionic pairs can not compete with solvation in solution.[3a]

On the other hand, all the *nido*-carborane-based compounds in Figure 1b show either the parallel or perpendicular orientation in the crystalline state (Figures 2a-c). In particular, the distance (centroid to centroid) and the dihedral angle (plane of π system and the open face C_2B_3 of *nido*-carborane) vary significantly, indicating the dependence on substituents at pyridinium and the type of aromatic rings (Figure S3). Firstly, compound **1-py** adopts less distorted parallel-displaced configuration in comparison to compounds **1-py-cn** and **1-py-ome** owing to the larger substituent effect in the π systems of the latter two compounds (Figure 2a). As such, a shorter distance of *nido*-cage···π interaction with 4.621 Å is observed for compound **1-py** than those of **1-py-cn** (4.995 Å) and **1-py-ome** (4.862 Å). Note that the three dimensional size of *nido*-carborane approaches 5.6 Å (Figure S4), thus the contacting distance formed in the ionic pairs in this study should be longer than the conventional non-covalent interactions,

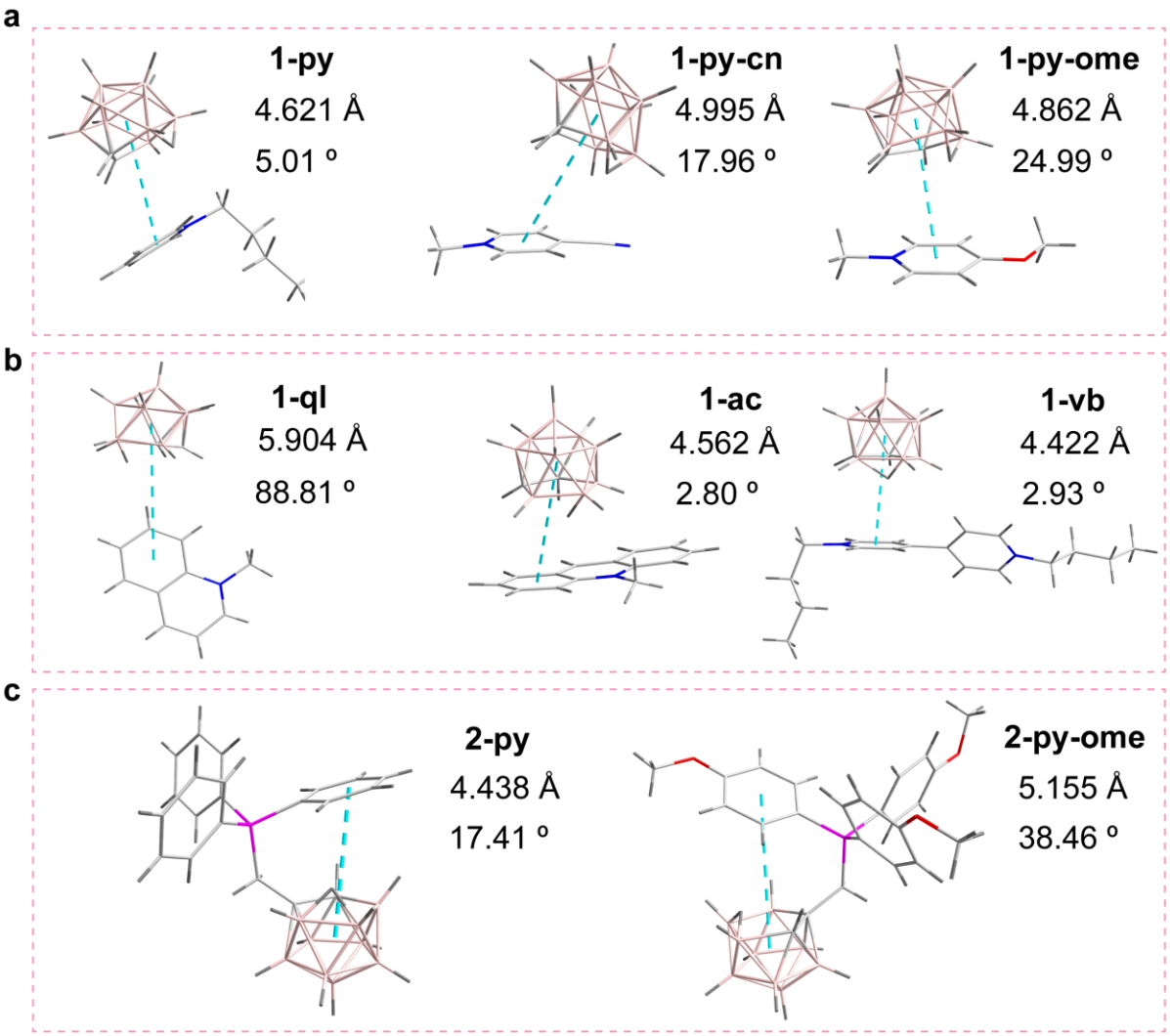

Figure 2. The crystal structures of *nido*-carborane-based compounds containing *nido*-cage···π interactions.

for example, beyond the range of π···π interactions (usually below 4.0 Å[5]). Correspondingly, the dihedral angle of 5.01° for **1-py** is smaller than those of 17.96° for **1-py-cn** and 24.99° for **1-py-ome**. Secondly, the packing mode can be tuned by the type of aromatic rings. Compound **1-ql** affords a T-shaped orientation between the *nido*-carboranyl cage and methylquinolinium (Figure 2b). This arrangement is similar to one of the standard π···π stacking interactions. Besides, this packing mode induces a much longer contacting distance (5.904 Å) than that of compound **1-py** (4.621 Å). In the case of **1-ac** with a larger conjugated acridinium, the face-to-face geometry with the *nido*-carboranyl unit is observed in the unit cell. This packing structure causes even a shorter contacting distance (4.562 Å) and smaller dihedral angle (2.8°) of the *nido*-cage···π interaction in comparison to **1-py** (4.621 Å and 5.01°). Unexpectedly, the cation N,N'-dibutyl-4,4'-bipyridinium, a strong electronic acceptor,[9] leads to the shortest contacting distance (4.422 Å) of *nido*-cage···π interaction in **1-vb** among the compounds in this study. Particularly, the unit cell contains two different conformations of the cation. One cation bearing a cage···π interaction possesses a twisted bipyridinium, whereas the other shows a planar configuration for the bipyridinyl unit which is surrounded by *nido*-carboranyl moieties through multiple B–H···H–C interactions (Figures S3f and S3g). DFT calculations reveal that the twisted cation is 1.3 kcal mol^{-1} lower than the planar one, a value close to those reported for biphenyl.[10] Obviously, the *nido*-cage···π interaction is devoted to the formation of more stable molecular conformation in the crystalline state.

With the aim to prove that the *nido*-cage···π interaction may not be predominated by electrostatic interaction between the boron cluster and the π system, we replaced pyridinium by a phenyl ring as a π system through removal of the positive charge from the nitrogen atom of pyridinium to the phosphorus atom of the phosphorium as shown in **2-py** (Figure 2c). In addition, the substituent effect is also considered by attachment of a methoxy group to the phenyl ring (e.g. **2-py-ome**). The crystal structure of compound **2-py** presents an intramolecular cage···π interaction between the *nido*-carboranyl cage and the phenyl ring with a contacting distance of 4.438 Å and a dihedral angle of 17.41° (Figure 2c). However, compound **2-py-ome** displays a twisted geometry with a longer contacting

distance of 5.155 Å and larger dihedral angle of 38.46º, fully reflecting the substituent effect as found in the intermolecular *nido*-cage···π interaction. Therefore, it is concluded that a *nido*-cage···π interaction can be generally existent, regardless of the type of aromatic rings and their substituents, as well as either intramolecular or intermolecular mode to be considered.

Quantum-chemical computations on *nido*-cage···π interaction

To better understand the nature of the *nido*-cage···π interaction observed, quantum chemical calculations based on the above crystal structures have been performed. Geometry optimized structures (Figure 3 and Table S2) at the ZORA-BLYP-D3BJ/TZ2P level of theory (see Supporting Information for full computational details) show a good agreement with the crystal geometries, i.e. the same parallel or perpendicular orientations are obtained with just some small conformation changes that we attribute to crystal packing effects. Nonetheless, the computed centroid to centroid distance somehow differs from that of the crystal structure. The best agreement is afforded for systems **2-py** and **2-py-ome** (*vide infra*) in which the *nido*-carboranyl unit and the π-system are intramolecularly linked. In the case of **1-ql**, the X-ray structure shows the fused benzene ring in T-shaped conformation versus the C_2B_3 ring of carborane, but in our calculations the system is relaxed to a displaced parallel conformation as observed in Figure 3.

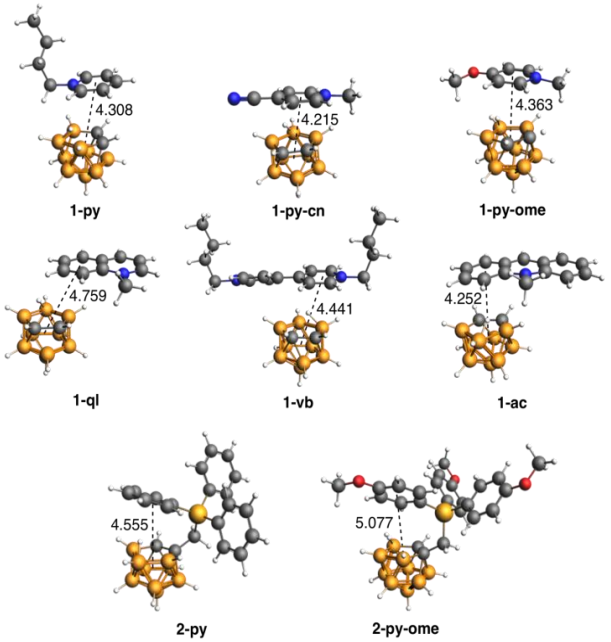

Figure 3. Set of optimized *nido*-cage···π systems under analysis. Computed distances (from the center of the π ring to the center of the carborane, in Å) between fragments are enclosed.

Next, a quantitative energy decomposition analysis (EDA, see Supporting Information for details) has been performed to characterize the interaction between the two fragments, i.e. *nido*-carborane and the π system (Table 1). The total bonding energies (ΔE) of the systems between *nido*-carborane and aryl-substituted pyridine (or quinoline or acridine) enclosed in Table 1 are in the order of -65 – -84 kcal mol^{-1}. System **1-vb** presents a stronger interaction because of its different characteristics (doubly cationic). Again, if we first focus on the former set of the five systems, the strain energy (energy required to deform the two reactants from their equilibrium structure to the geometry they adopt in the complex) is small in all cases (maximum of 1.9 kcal mol^{-1}), which means that the interaction between the two species hardly affects the geometry of the relaxed fragments at infinite distance. Then, the interaction energy (ΔE_{int}) can be further decomposed into Pauli (ΔE_{Pauli}), electrostatic (ΔV_{elstat}), orbital interaction (ΔE_{oi}), and dispersion terms (ΔE_{disp}).[11] In particular, the fact that *nido*-carborane is negatively charged, whereas the N-hetero-ring is positively charged, causes the interaction between the two fragments to be mainly electrostatic ($\%_{elstat} = \Delta V_{elstat}/(\Delta V_{elstat}+\Delta E_{oi}+\Delta E_{disp})$), which is in the order of 65–72%, in front of the much minor covalent contribution. It must be pointed out that even though **1-vb** presents different characteristics of the system interacting with *nido*-carborane, the interaction is also mainly electrostatic (71%).

Table 1. Energy decomposition analysis (EDA) (in kcal mol^{-1}) of the systems.

System	ΔE	ΔE_{strain}	ΔE_{int}	ΔE_{Pauli}	ΔV_{elstat}	ΔE_{oi}	ΔE_{disp}	$\%_{elstat}$
1-py	-73.1	0.4	-73.5	23.2	-68.5	-14.4	-13.8	*71*
1-py-ome	-73.7	1.1	-74.8	24.8	-72.0	-12.9	-14.7	*72*
1-py-cn	-83.7	1.9	-85.6	29.4	-74.8	-25.4	-14.7	*65*
1-ql	-64.8	1.3	-66.1	17.9	-58.5	-15.0	-10.4	*70*
1-vb	-135.8	3.7	-139.5	29.3	-119.1	-32.0	-17.6	*71*
1-ac	-70.4	1.6	-72.0	23.4	-61.8	-18.1	-15.6	*65*

With the aim to compare the above discussed boron cluster-π interactions with π-π interactions present in well-known classical aromatic species, we have taken system **1-py** as the reference, and performed a systematic analysis for the systems depicted in Figure 4. In particular, we have first changed butyl-pyridine by pyridine and benzene, and then the carborane has been changed by benzene and cyclopentadienyl anion. Interestingly, the structure of $(C_2B_9H_{11})Fe(C_5H_5)$, a metallocarborane derivative (shown in Figure 1b) reported by Hawthorne,[12] indicates that $C_2B_9H_{12}^-$ and $C_5H_5^-$ share similar chemical bonding characteristics. Indeed, there are five molecular orbitals in $C_2B_9H_{12}^-$ with similar shapes and energies as the five π molecular orbitals of $C_5H_5^-$ (Figure S18), with the cyclopentadienyl anion having slightly less stable MOs and, therefore, higher electron donating character. The optimized geometries enclosed in Figure 4 show the parallel displaced equilibrium geometries for all systems, except when either neutral pyridine or benzene interacts with the negatively charged *nido*-carborane or the cyclopentadienyl anion (systems **1b**, **1c**, **1h**, and **1i**), in which case the T-shaped conformation is preferred. With respect to system **1f**, i.e. benzene dimer, the calculated results at either ZORA-revPBE-D3BJ/TZ2P or ZORA-BLYP-D3BJ/TZ2P are in agreement with previously reported data at higher levels of theory showing that the parallel displaced (PD), the T-shaped tilted (TT) and the T-shaped (T) conformations are almost isoenergetic.[13] In our ZORA-BLYP-D3BJ/TZ2P calculations, the PD con-

formation is the most stable, followed by the TT at 0.32 kcal mol^{-1}, the T at 0.52 kcal mol^{-1}, and finally the sandwich (S) at 1.14 kcal mol^{-1} (Table S3).

The EDA analysis performed on this set of systems (Table S5) shows the importance of dealing with charged species or neutral ones at determining the character of the interaction between the two fragments. Thus, when the two fragments are neutral (**1f** and **1e**), the dispersion (ΔE_{disp}) is the most attractive term of the interaction energy (ΔE_{int}). For charged species, the interaction energy is much higher by a factor of about 10 and the electrostatic term (ΔV_{elstat}) becomes the most important. It should be noted at this point that the nature of the interaction between **1-py** and **1g** (i.e., changing $C_2B_9H_{12}^-$ by $C_5H_5^-$) is basically the same, the electrostatic component being the most important followed by the orbital interaction (ΔE_{oi}) and the dispersion terms. The higher interaction of **1g** is ascribed to the larger HOMO-LUMO overlap in this system (Table S6 and Figure S7), which results in larger ΔE_{oi} and, consequently, shorter distance between the fragments. The latter is translated in higher repulsive Pauli repulsions and larger attractive ΔV_{elstat} interactions. Similarly, the interactions in **1c** and **1i** or in **1b** and **1h** are of the same nature, which proves that the C_2B_3 ring of $C_2B_9H_{12}^-$ interacts with pyridine (**1b**) or benzene (**1c**) almost identically to the cyclopentadienyl anion in **1h** or **1i**. It fully proves that *nido*-carborane can be treated as a building block to form these new non-covalent intermolecular interactions.

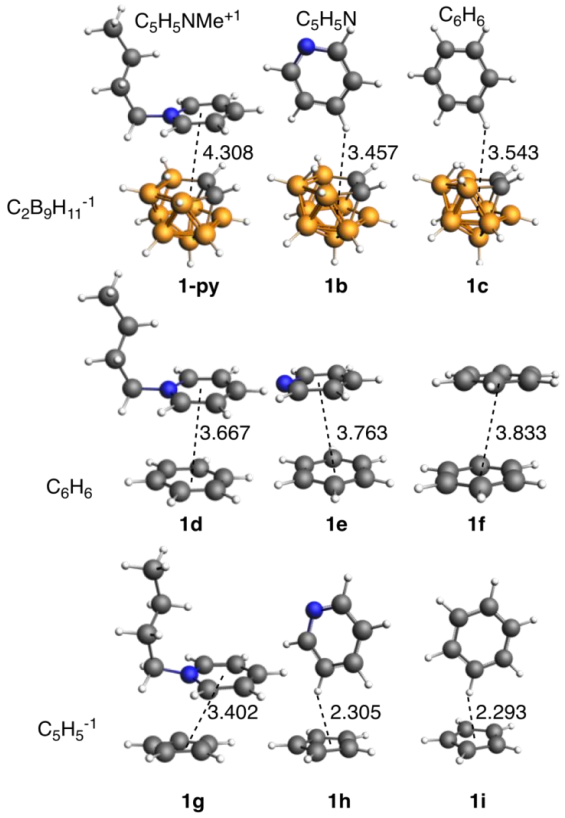

Figure 4. Set of derived systems from compound **1-py**. Computed distances (in Å) between fragments are enclosed.

To further clarify that this *nido*-cage-π bond is not a pure electrostatic interaction, we have performed an EDA analysis for system **1-ac** and its derived systems **ac-s** (SbF_6^-), **ac-p** (PF_6^-), and **ac-b** (BF_4^-) (Figures 5a and S9 and Table S8), in which *nido*-carborane is substituted by fluorinated anion species. Our results indicate that the components of the interaction energy are quite similar for these four systems. However, for **1-ac**, the electrostatic term is somewhat less attractive than in the rest of the systems because the negative charge is more delocalized whereas the orbital interaction and dispersion terms are more attractive because of the existence of the *nido*-cage-π interaction. Finally, we have analyzed the two systems with intramolecular *nido*-cage-π interaction enclosed in Figure 2 (**2-py** and **2-py-ome**). Results obtained indicate that the trends remain the same no matter if the *nido*-cage-π interaction is inter or intramolecular (Table S10).

Variable photophysical properties triggered by *nido*-cage···π interaction

To explore the properties and potential applications of the new non-covalent *nido*-cage···π interaction, a set of experiments were conducted on the selected compound **1-ac**, and the fluorinated ionic pairs **ac-s**, **ac-p**, and **ac-b** were used as model systems (Figure 5a). First of all, we investigated the electronic properties of these compounds to try to uncover the influence from *nido*-cage···π interactions. The absorption spectra in THF indicates no evident difference between **1-ac** and the model compound **ac-p** (Figure S19), demonstrating that the attractive interaction for the ionic pairs in solution can not change the ground state of methylacridinium as shown in the NMR spectra in solution. However, a large red-shift (~110 nm) in the absorption spectra is observed in the solid state (Figure S20). This bathochromic-shift transition can be assigned to a charge transfer (CT) transition between the two fragments.[9] The CT character of the ground state for **1-ac** is verified by the solid-state electron paramagnetic resonance (EPR) spectrum[14] (Figure S21). A relatively weak but sharp resonance signal is centered at 3324 T, indicating the existence of an active radical. The g factor is calculated to be 2.0029, which is almost equal to the value of a free electron (2.0023). But no EPR signal is detected for compound **ac-s**. In addition, the theoretical calculations at the CAM-B3LYP/TZ2P level also suggest a new CT absorption band for **1-ac** (Figures S13-17 and Table S11). Particularly, such a CT transition is not observed in either methylacridinium or the control compounds **ac-s**, **ac-p**, and **ac-b**. Indeed, the *nido*-cage···π interaction influences the ground state properties in solid state.

To further support the electronic communication between *nido*-carborane and methylacridinium, the photophysical properties in the excited states for **1-ac** and the control compounds **ac-s**, **ac-p**, and **ac-b** were tested as well. The band positions in the PL (photoluminescence) spectra for **1-ac** and **ac-p** in THF are the same (Figure 5b). However, the luminous efficiency of compound **1-ac** (66.06%) is lower than that of compound **ac-p** (91.94%), which indicates the existence of extra non-radiative channel in the excited states for **1-ac**. Unexpectedly, compound **1-ac** shows ACQ in the crystalline state in contrast to the low luminous efficiencies of compounds **ac-s**, **ac-p**, and **ac-b** (Figures 5c and S22). This could be attributed to the multiple and face to face π···π interactions in the packing structures of the latter compounds (see Figure 5d),

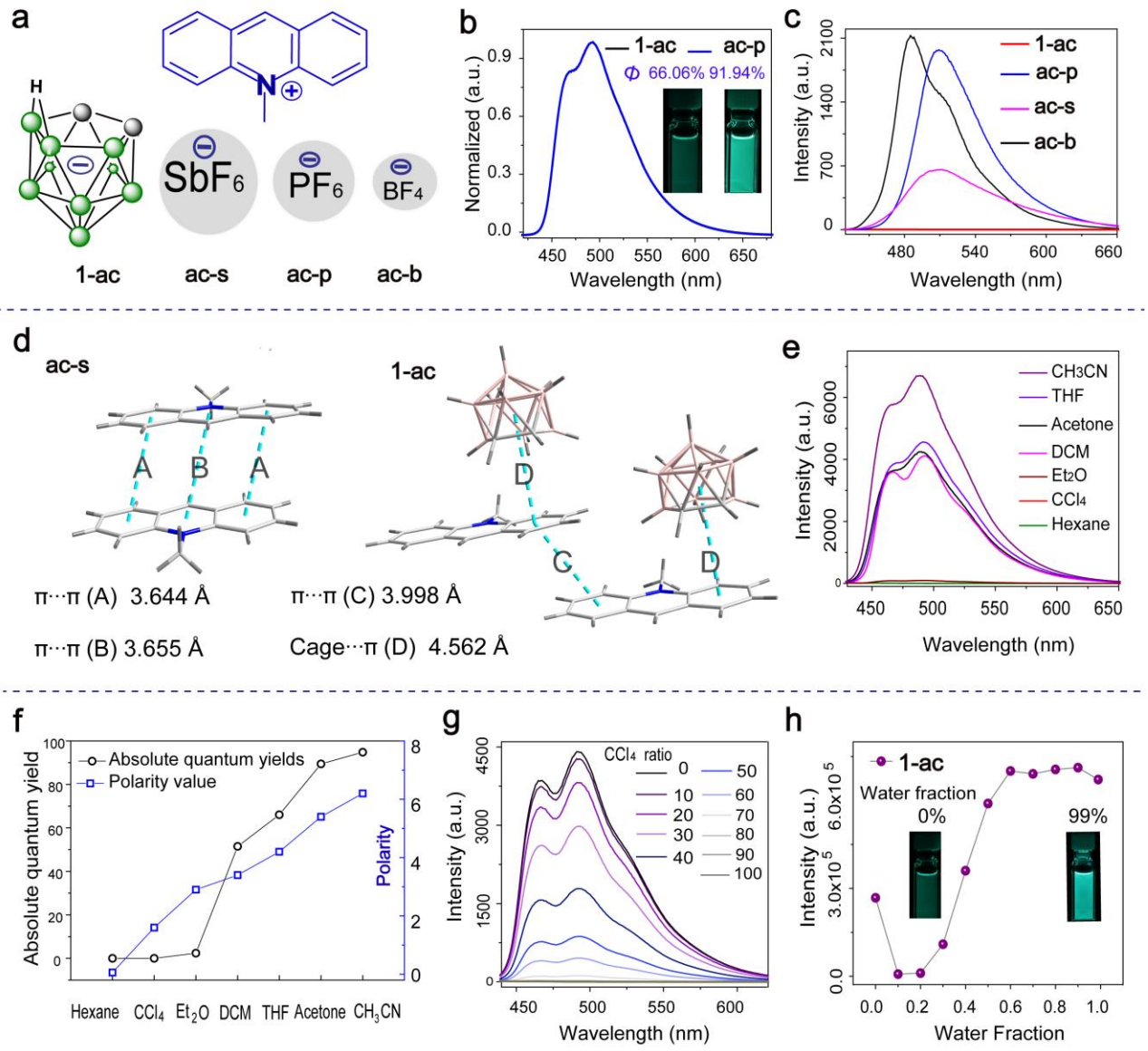

Figure 5. Variable photophysical properties triggered by *nido*-cage···π interaction. a) Schemed structures for **1-ac**, **ac-s**, **ac-p**, and **ac-b**. b) PL spectra of **1-ac** and **ac-p** in THF. Inset: luminescence photographs. c) PL spectra of **1-ac**, **ac-s**, **ac-p**, and **ac-b** in solid state. d) The packing structures of **1-ac** and **ac-s**. e) PL spectra of **1-ac** in different solvents. f) The absolute quantum yields of **1-ac** in different solvents. g) PL spectra of **1-ac** in different fractions of CH_2Cl_2 and CCl_4. h) The luminescent intensity for different water fractions.

which prompts the formation of such rigid and detrimental species as excimers,[15] thus leading to the observed low luminous efficiency in solid state. In the case of **1-ac**, however, the packing structure is totally different, where only the *nido*-cage···π interaction (4.562 Å) and the negligible π···π interaction (3.998 Å) are observed (Figure 5d). Therefore, we infer that such a packing style is induced by the *nido*-cage···π interaction, which leads to luminescence quenching for **1-ac** in crystalline state.

The further investigation on PL spectra in solution for **1-ac** was performed as an ionic species facilely influenced by media. Firstly, the PL spectra in different solvents (Figure 5e) show that the emission band positions in the range of 450-600 nm remain unchanged, reflecting the characteristic π–π* transition of the methylacridinium fragment. However, the luminous efficiency is sharply dependent on solvent polarity. In particular, in the non-polar or less polar solvents such as CCl_4 and hexane, no luminescence can be detected, showing the same phenomenon as in crystalline state. If the solvent polarity is increased, the absolute quantum yield is correspondingly improved (Figure 5f). The similar result is also observed in the mixed solvents of CH_2Cl_2 and CCl_4 (Figures 5g and S23). Therefore, we assume that in the low polar solvents compound **1-ac** forms compact ionic pairs to create CT complexes, thus leading to luminescence quenching. When the compound is dissolved in polar solvents, the compact ionic pair can be

dissociated, thus luminescence is regenerated. Secondly, the PL spectra in the mixed solvents of THF and water demonstrate aggregation-induced emission (AIE)[15] during addition of water (Figures 5h and S24). The X-ray powder diffraction indicates the formation of amorphous particles upon water fraction up to 99% (Figure S25). Clearly, in the amorphous state, the *nido*-cage···π interaction can be destroyed. On the basis of these results, it is easily understood that the formation of *nido*-cage···π interaction requires a crystalline atmosphere. Only in crystalline form can effective electronic communication be induced. In summary, the luminescent properties of the zwitterionic species such as **1-ac** can be tuned by both solvent polarity and the condensed state form, showing variable photophysical properties for one molecule.

Conclusions

For the first time, a novel type of non-covalent interaction, boron-cluster cage···π interaction has been experimentally discovered in both intramolecular and intermolecular modes. Theoretical calculations reveal a major electrostatic character or orbital- and dispersion-dominated interaction, similar to those found in cyclopentadienyl anion···π or π···π interactions. In this study, the *nido*-cage···π interaction has been successfully used to tune both ground state and excited state properties of organic luminogens. These findings not only extend the types of non-covalent bonds and strengthen the understanding on non-covalent interactions, but also open a door to exploit the *nido*-cage···π interaction for self-assembly, luminescent materials, and other potential applications.

ASSOCIATED CONTENT

Supporting Information contains the following contents such as experimental details, photophysical properties, X-ray structures of *nido*-carborane-based compounds (CIFs), NMR, MS spectra, a detailed description of quantum chemical methods used, Cartesian coordinates of all optimized species, benchmark studies, and additional energy decomposition analyses. This material is available free of charge via the Internet at http://pubs.acs.org.

AUTHOR INFORMATION

Corresponding Author

E-mail: hyan1965@nju.edu.cn (H. Y.)
miquel.sola@udg.edu (M. S.)
jordi.poater@ub.edu (J. P.)

ACKNOWLEDGMENT

This work has been supported by the Ministerio de Economía y Competitividad (MINECO) of Spain (Projects CTQ2017-85341-P, CTQ2016-77558-R, and MDM-2017-0767) and the Generalitat de Catalunya (projects 2017SGR39 and 2017SGR348, and ICREA Academia 2014 prize for M.S.). Excellent service by the Supercomputer center of the Consorci de Serveis Universitaris de Catalunya (CSUC) is gratefully acknowledged. The authors also gratefully acknowledge the financial support from NSFC (21820102004 and 21531004).

REFERENCES

[1] a) Dyker, C. A.; Bertrand G. Chemical bonding: rethinking carbon. *Nature Chem.* **2009**, *1*, 265-301. b) Dawson R. E.; Hennig, A.; Weimann, D. P.; Emery, D.; Ravikumar, V.; Montenegro, J.; Takeuchi, T.; Gabutti, S.; Mayor, M.; Mareda, J.; Schalley, C. A.; Matile, S. Experimental evidence for the functional relevance of anion-π interactions. *Nature Chem.* **2010**, *2*, 533-538. c) Zhao, L. L.; Hermann, M.; Schwarz, W. H. E.; Frenking, G. The Lewis electron-pair bonding model: modern energy decomposition analysis. *Nature Rev. Chem.* **2019**, *3*, 48-63.

[2] a) Zhang, Q.; Li, T.; Duan, A.; Dong, S.; Zhao, W.; Stang, P. J. Formation of a supramolecular polymeric adhesive via water-participant hydrogen bond formation. *J. Am. Chem. Soc.* **2019**, *141*, 8058−8063. b) Yu, G.; Zhang, M.; Saha, M. L.; Mao, Z.; Chen, J.; Yao, Y.; Zhou, Z.; Liu, Y.; Gao, C.; Huang, F. H.; Chen, X. Y.; Stang, P. J. Antitumor activity of a unique polymer that incorporates a fluorescent self-assembled metallacycle. *J. Am. Chem. Soc.* **2017**, *139*, 15940-15949. c) Li, E.; Jie, K.; Zhou Y.; Zhao R.; Huang, F. H. Post-synthetic modification of nonporous adaptive crystals of pillar[4]arene[1]quinone by capturing vaporized amines. *J. Am. Chem. Soc.* **2018**, *140*, 15070-15079. d) Burley, S. K.; Petsko, G. A. Aromatic-aromatic interaction: a mechanism of protein-structure stabilization. *Science* **1985**, *229*, 23-28. e) Aida, T.; Meijer, E. W.; Stupp, S. I. Functional supramolecular polymers. *Science* **2012**, *335*, 813-81. f) Mahadevi, A. S.; Sastry, G. N. Cation-π interaction: its role and relevance in chemistry, biology, and material science. *Chem. Rev.* **2012**, *113*, 2100-2138

[3] a) Wang, D. X.; Wang, M. X. Anion-π interactions: generality, binding strength, and structure. *J. Am. Chem. Soc.* **2013**, *135*, 892-897. b) Liu, H.; Zhang, Q.; Wang, M. X. Synthesis, structure, and anion binding properties of electron-deficient tetrahomocorona[4]arenes: shape selectivity in anion-π interactions. *Angew. Chem. Int. Ed.* **2018**, *57*, 6536-6540. c) Tsuzuki, S.; Honda, K.; Uchimaru, T.; Mikami, M.; Tanabe, K. Origin of the attraction and directionality of the NH/π interaction: comparison with OH/π and CH/π interactions. *J. Am. Chem. Soc.* **2000**, *122*, 11450-11458. d) Ma, J. C.; Dougherty, D. A. The cation−π interaction. *Chem. Rev.* **1997**, *97*, 1303-1324. e) Cavallo, G.; Metrangolo, P.; Milani, R.; Pilati, T.; Priimagi, A.; Resnati, G.; Terraneo, G. The halogen bond. *Chem. Rev.* **2016**, *116*, 2478-2601. f) Aakeröy, C. B.; Seddon, K. R. The hydrogen bond and crystal engineering. *Chem. Soc. Rev.* **1993**, 22, 397-407.

[4] a) Zou, W.; Zhang, X.; Dai, H.; Yan, H., Cremer, D.; Kraka, E. Description of an unusual hydrogen bond between carborane and a phenyl group. *J. Organomet. Chem.* **2018**, *865*, 114-127. b) Bhattacharyya, P. B-H_b···π interactions in benzene-borazine sandwich and multidecker complexes: a DFT study. *New J. Chem.* **2017**, *41*, 1293-1302. c) Fanfrlik, J.; Pecina, A.; Řezáč, J.; Sedlak, R.; Hnyk, D.; Lepšík, M.; Hobza, P.; B-H···π: a nonclassical hydrogen bond or dispersion contact? *Phys. Chem. Chem. Phys.* **2017**, *19*, 18194-18200. d) Fox M. A.; Hughes, A. K. Cage C–H···X interactions in solid-state structures of icosahedral carboranes, *Coord. Chem. Rev.* **2004**, *248*, 457-476. e) Raston, C. L.; Cave, G. W. V. Nanocage encapsulation of two ortho-carborane molecules. *Chem. Eur. J.* **2004**, *10*, 279-282. f) Bakar, M. A.; Sugiuchi, M.; Iwasaki, M.; Shichibu, Y.; Konishi, K. Hydrogen bonds to Au atoms in coordinated gold clusters. *Nat. Commun.* **2017**, *8*, 576. g) Frontera, A.; Bauzá, A. closo-Carboranes as dual CH···π and BH···π donors: theoretical study and biological significance. *Phys. Chem. Chem. Phys.* **2019**, *21*, 19944-19950.

[5] a) Meyer, E. A.; Castellano R. K.; Diederich, F. Interactions with aromatic rings in chemical and biological recognition. *Angew. Chem. Int. Ed.* **2003**, *42*, 1210-1250. b) Pearcy, A. C.; Mason, K. A.; El-Shall, M. S. Ionic Hydrogen and Halogen bonding in the gas phase association of acetonitrile and acetone with halogenated benzene cations. *J. Phys. Chem. A* **2019**, *123*, 1363-1371.

[6] a) Tsuzuki, S.; Honda, K.; Uchimaru, T.; Mikami, M.; Tanabe K. Origin of attraction and directionality of the π/π interaction: model chemistry calculations of benzene dimer interaction. *J. Am. Chem. Soc.* **2002**, *124*, 104-112. b) Sinnokrot, M.; Valeev, E. F.; Sherrill, C.

D. Estimates of the ab initio limit for π-π interactions: the benzene dimer. *J. Am. Chem. Soc.* **2002**, *124*, 10887-10893.
[7] a) Hosmane, N. S. Boron science: new technologies and applications, CRC Press, Boca Raton, FL, **2011**. b) Williams, R. E. The polyborane, carborane, carbocation continuum: architectural patterns. *Chem. Rev.* **1992**, *92*, 177-207. c) Wang, H.; Wu, L.; Lin, Z. Y.; Xie, Z. W. Synthesis, structure and reactivity of a borylene cation $[(NHSi)_2B(CO)]^+$ stabilized by three neutral ligands. *J. Am. Chem. Soc.* **2017**, *139*, 13680-13683. d) Buades, A. B.; Arderiu, V. S.; Olid-Britos, D.; Viñas, C.; Sillanpaä, R.; Haukka, M.; Fontrodona, X.; Paradinas, M.; Ocal, C.; Teixidor, F. Electron accumulative molecules. *J. Am. Chem. Soc.* **2018**, *140*, 2957-2970. e) Núñez, R.; Romero, I.; Teixidor, F.; Viñas, C. Icosahedral boron clusters: a perfect tool for the enhancement of polymer features. *Chem. Soc. Rev.* **2016**, *45*, 5147-5173.
[8] a) Grimes, R. N. Carboranes, Academic Press, New York, 3rd edition, **2016**. b) Scholz, M.; Hey-Hawkins, E. Carbaboranes as pharmacophores: properties, synthesis, and application strategies. *Chem. Rev.* **2011**, *111*, 7035-7062. c) King R. B. Three-dimensional aromaticity in polyhedral boranes and related molecules. *Chem. Rev.* **2001**, *101* 1119-1152. d) Longuet-Higgins, H. C. Substances hydrogénées avec défaut d'électrons. *J. Chim. Phys.* **1949**, *46*, 268-275. e) Eberhardt, W. H.; Crawford Jr., B.; Lipscomb, W. N. The valence structure of the boron hydrides. *J. Chem. Phys.* **1954**, *22*, 989-1001. f) Lipscomb, W. N. The boranes and their relatives. *Science* **1977**, *196*, 1047-1055. g) Poater, J.; Solà, M.; Viñas, C.; Teixidor, F. π aromaticity and three-dimensional aromaticity: two sides of the same coin? *Angew. Chem. Int. Ed.* **2014**, *53*, 12191-12195. h) Poater, J.; Solà, M.; Viñas, C.; Teixidor, F. *Chem. Eur. J.* Hückel's rule of aromaticity categorizes aromatic closo boron hydride clusters. **2016**, *22*, 7437-7443. i) Poater, J.; Solà, M.; Viñas, C.; Teixidor, F. A simple link between hydrocarbon and borohydride chemistries. *Chem. Eur. J.* **2013**, *19*, 4169-4175.
[9] Yu, W.; Wang, X. Y.; Li, J.; Li, Z. T.; Yan, Y. K.; Wang, W.; Pei, J. A photoconductive charge-transfer crystal with mixed-stacking donor-acceptor heterojunctions within the lattice. *Chem. Comm.* **2013**, *49*, 54-56.
[10] a) Poater, J.; Solà, M.; Bickelhaupt, F. M. Hydrogen–Hydrogen bonding in planar biphenyl, predicted by atoms-in-molecules theory, does not exist. *Chem. Eur. J.* **2006**, *12*, 2889-2895. b) Johansson, M. P.; Olsen, J. torsional barriers and equilibrium angle of biphenyl: reconciling theory with experiment. *J. Chem. Theory Comput.* **2008**, *4*, 1460-1471.
[11] a) Bickelhaupt, F. M.; Diefenbach, A.; de Visser, S. P.; de Koning, L. J.; Nibbering, N. M. M. Nature of the three-electron bond in $H_2S\therefore SH_2^+$. *J. Phys. Chem. A* **1998**, *102*, 9549-9553. b) Bickelhaupt, F. M.; Baerends, E. J. in Reviews in Computational Chemistry, Vol. 15 (Eds.: Lipkowitz, K. B.; Boyd, D. B.), Wiley-VCH, New York, **2000**, pp. 1-86; c) Wolters, L. P.; Bickelhaupt, F. M. The activation strain model and molecular orbital theory. *WIRES Comput. Mol. Sci.* **2015**, *5*, 324-343. d) von Hopffgarten, M.; Frenking, G. Energy decomposition analysis. *WIRES Comput. Mol. Sci.* **2011**, *2*, 43.
[12] Hawthorne M. F. Chemistry of the polyhedral species derived from transition metals and carboranes. *Acc. Chem. Res.* **1968**, *1*, 281-288.
[13] a) Pitonák, M.; Neogrády, P.; Rezác, J.; Jurecka, P.; Urban, M.; Hobza, P; Benzene dimer: high-level wave function and density functional theory calculations. *J. Chem. Theor. Comput.* **2008**, *4*, 1829-1834. b) Schnell, M.; Erlekam, U.; Bunker, P. R.; Helden, G. v.; Grabow J. U.; Meijer, G.; Avoird, A. Structure of the benzene dimer-governed by dynamics. *Angew. Chem. Int. Ed.* **2013**, *52*, 5180-5183; Smith, T.; Slipchenko, L. V.; Gordon, M. S. Modeling π–π interactions with the effective fragment potential method: the benzene dimer and substituents. *J. Phys. Chem. A* **2008**, *112*, 5286-5294.
[14] Zhu, W.; Zheng, R. H.; Fu, X. L.; Fu, H. B.; Shi, Q.; Zhen, Y. G.; Dong, H.; Hu, W. P. Revealing the charge-transfer interactions in self-assembled organic cocrystals: two-dimensional photonic applications. *Angew. Chem. Int. Ed.* **2015**, *54*, 6785-6789.
[15] Hong, Y.; Lam, J. W. Y.; Tang, B. Z. Aggregation-induced emission. *Chem. Soc. Rev.* **2011**, *40*, 5361-5388.

TOC

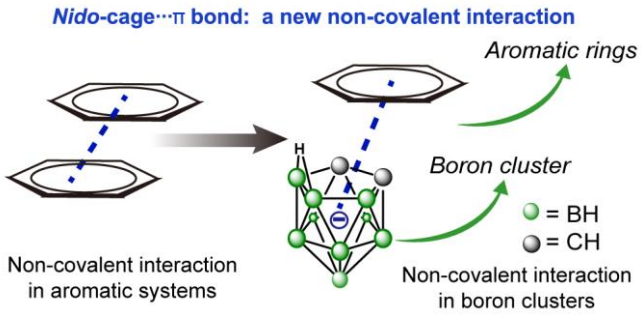
Nido-cage···π bond: a new non-covalent interaction
Aromatic rings
Boron cluster
= BH
= CH
Non-covalent interaction
in aromatic systems
Non-covalent interaction
in boron clusters